Decentralized Policy Gradients for Optimizing Generalizable Policies in Multi-Agent Reinforcement Learning

Anonymous authors
Paper under double-blind review

Abstract

Parameter Sharing (PS) is a widely used practice in Multi-Agent Reinforcement Learning (MARL), where a single neural network is shared among all agents. Despite its efficiency and effectiveness, PS can occasionally result in suboptimal performance. While prior research has primarily addressed this issue from the perspective of update conflicts among different agents, we investigate it from an optimization standpoint. Specifically, we point out the analogy between PS in MARL and Centralized SGD (CSGD) in distributed learning and hypothesize that PS may inherit similar convergence and generalization issues as CSGD, such as lower convergence levels of key metrics and larger generalization gaps. To address these issues, we propose Decentralized Policy Gradients (DecPG), which leverages the principles of Decentralized SGD. We use an environment with additional noise injected into the observation and action spaces to evaluate the generalization of DecPG. Empirical results show that DecPG outperforms its centralized counterpart, PS, across various aspects—achieving higher rewards, smaller generalization gaps, and flatter reward landscapes. The results confirm that PS suffers from convergence and generalization issues similar to those of CSGD, and show that our DSGD-based method, DecPG, effectively mitigates these problems—offering a new optimization perspective on MARL algorithm performance.

1 Introduction

In cooperative Multi-Agent Reinforcement Learning (MARL), multiple agents interact cooperatively with each other and with the environment to achieve a common goal. Each agent has an individual policy, and together they form a joint policy. MARL algorithms aim to train this joint policy to maximize the return. A typical practice to optimize the joint policy is Parameter Sharing (PS) (Gupta et al., 2017; Chu & Ye, 2017; Terry et al., 2020b; Yu et al., 2022; Rashid et al., 2020). Instead of training a separate neural network for each agent policy, PS employs a single shared network for all agents. It is simple to implement, and training one shared policy with data from all agents offers promising sample efficiency. Because of these advantages, PS has been adopted in various benchmark algorithms, such as MAPPO (Yu et al., 2022) and QMix (Rashid et al., 2020).

Interestingly, the PS in MARL shares great similarities with the centralized SGD (CSGD) used in distributed learning. In particular, distributed learning trains deep neural networks at scale by leveraging parallel training across multiple nodes. Each node maintains a copy of the initial model and has access to a local dataset, allowing it to perform gradient descent locally. In CSGD, there is a central parameter server that aggregates the updates from local nodes and broadcasts the aggregated results back to all nodes, corresponding exactly to the update style of PS. This approach is essentially equivalent to single-worker SGD, but its distributed nature allows CSGD to parallelize the computation across multiple nodes, enabling larger effective batch sizes and significantly improving training efficiency (Dekel et al., 2012).

This analogy between PS and CSGD intrigues us to investigate whether PS inherits similar optimization issues from CSGD. Particularly, CSGD faces several optimization challenges in practice, including convergence to suboptimal loss levels or complete failure to converge with large batches (Zhang et al., 2019; You et al., 2017; Jastrzebski et al., 2017), and poorer generalization (Goyal et al., 2017; Keskar et al., 2016). PS has also been found to result in suboptimal performance in several experiments, including both heterogeneous and homogeneous agent settings (Kim & Sung, 2023; Qin et al., 2025). Most existing papers address the problem from only one perspective—by mitigating the conflicting updates among different agents, for instance, via improving the parameter sharing mechanism, as in SePS (Christianos et al., 2021) and SNP-PS (Kim & Sung, 2023), or utilizing sequential training, like HAPPO (Zhong et al., 2024) and A2PO (Wang et al., 2023). However, alternative perspectives, particularly from the connection between PS and CSGD, remain largely underexplored.

On the other hand, this connection can offer a novel understanding of the performance limitations of PS in MARL and provide insights to address them. Crucially, in CSGD, one effective way to address the aforementioned problems is to shift from a centralized framework to a decentralized one, i.e., Decentralized SGD (DSGD) (Lian et al., 2017; Zhang et al., 2021; Zhu et al., 2023), which eliminates the need for a central server to perform update averaging and requires only local aggregation at each node with its neighbors defined by a *communication topology*. Although the local models are initialized with identical parameters, partial averaging causes the local models to diverge. This divergence introduces an intrinsic noise that acts as a regularization, smoothing the loss landscape and stabilizing training (Zhang et al., 2021). Theoretically and empirically, this noise has been shown to improve convergence and generalization relative to CSGD (Zhang et al., 2021; Zhu et al., 2023). Importantly, the benefits of DSGD do not diminish with increasing batch sizes.

Inspired by these findings, this paper investigates whether incorporating DSGD in MARL could effectively address these issues caused by PS. To this end, we propose **Decentralized Policy Gradient (DecPG)**, which incorporates DSGD's style of update into a policy-based MARL algorithm. We primarily focus on homogeneous agents, as they strongly correlates with the setting of distributed learning, where all nodes are treated equivalently. In the Multi-Agent Particles (MPE) Simple Spread (Mordatch & Abbeel, 2017) and StarCraft Multi-Agent Challenge (SMAC) (Samvelyan et al., 2019), we compare PS to DecPG with topologies from sparse to dense. We analyze how convergence and generalization behavior vary across these settings. Through comprehensive experiments, we empirically demonstrate that PS in MARL suffers from similar convergence and generalization issues as CSGD. The DSGD-based method, DecPG, mitigates these problems and outperforms PS, exhibiting behavior analogous to DSGD.

Our contributions are as follows.

- We propose DecPG—a policy gradient-based MARL algorithm built on DSGD—to improve convergence and generalization over its centralized counterpart, PS.
- We provide comprehensive empirical results to show that DecPG outperforms PS in training and test performance in most scenarios.
- We analyze the effect of communication topology sparsity—from sparse to dense—on final generalization performance. We evaluate a series of topologies whose spectral gaps span approximately linearly from 0 to 1, as defined by k-nearest-neighbor graphs. Our results show that the generalization capability tends to improve as the topology becomes sparser.
- We provide a qualitative visualization of the reward and loss landscapes for DecPG under topologies of varying sparsity, as well as for PS, showing that reward landscape smoothness improves from PS to DecPG as the topology becomes sparser.

2 Related Work

This paper investigates whether PS in MARL exhibits similar optimization problems as CSGD in distributed learning, and whether the proposed DSGD-based method, DecPG, can address these issues. Accordingly, this section reviews the related work about the characteristics and issues of PS and CSGD, and the recent developments in DSGD.

Parameter Sharing (PS) PS employs a single neural network to represent the policies of all agents, making it particularly efficient and scalable as the number of agents increases. With the inclusion of agent

ID (usually a one-hot encoding) to the input, PS can handle not only homogeneous but also heterogeneous problems (Terry et al., 2020a). It has been widely used in benchmark algorithms and has demonstrated outstanding empirical performance (Gupta et al., 2017; Chu & Ye, 2017; Terry et al., 2020b; Yu et al., 2022; Rashid et al., 2020). Despite its empirical success, PS has been found to be suboptimal in certain scenarios, including both homogeneous and heterogeneous settings (Kim & Sung, 2023; Qin et al., 2025). One direction to address it is by modifying the parameter sharing strategy, typically by making the neural network partially shared and partially specialized, rather than fully shared. These methods include SePS (Christianos et al., 2021), SNP-PS (Kim & Sung, 2023), Kaleidoscope (Li et al., 2024), GradPS (Qin et al., 2025), etc. The other direction focuses directly on the MARL algorithm itself, such as HAPPO/HATRPO (Zhong et al., 2024) and A2PO (Wang et al., 2023), utilizing sequential agent updates instead of simultaneous ones. These existing approaches aim to mitigate conflicts between different agents' updates. In contrast, this paper addresses this from an optimization perspective, a relatively unexplored direction in MARL.

Centralized SGD (CSGD) and Decentralized SGD (DSGD). In distributed learning, larger batch sizes are crucial for enhancing parallelism, but **CSGD** (or equivalently, single-worker SGD) is found to suffer from performance problems in large batch settings (You et al., 2017; Jastrzebski et al., 2017; Goyal et al., 2017; Zhang et al., 2019). Zhang et al. (2019) observe that using CSGD with batch sizes exceeding a certain threshold significantly deteriorates convergence, resulting in a high and non-decreasing training loss. This behavior is speculated to stem from a lack of stochasticity in the gradients. On the other hand, Goyal et al. (2017) discover an increasing trend in validation error with larger batch sizes, indicating a decline in generalization performance. Keskar et al. (2016) analyze this phenomenon from the perspective of optimization landscape flatness, where it is generally believed that flatter minima correspond to better generalization (Hochreiter & Schmidhuber, 1997). They empirically demonstrate that larger batch sizes tend to converge to sharper minima, whereas smaller batch sizes lead to flatter ones. **DSGD** was once considered a compromise to CSGD, viewed as useful only under poor bandwidth or high network latency. However, it has since been shown to outperform CSGD in large-batch training scenarios. Lian et al. (2017) prove that DSGD can achieve the same convergence rate as CSGD and exhibit a similar asymptotic linear speedup in computational complexity with respect to the number of nodes. This enables DSGD to converge in less wall-clock time than CSGD in practice, due to its significantly lower communication overhead on individual nodes. Koloskova et al. (2020) establish a unified framework that proves convergence guarantees for DSGD under different scenarios, including changing topologies, i.i.d. and non i.i.d. data distributions. Zhang et al. (2021) show that DSGD can lead to better convergence than CSGD due to the noise arising from the differences among the local model weights across nodes. This noise is dependent on the optimization landscape. Specifically, at early stages of training, when the gradients are large due to the relatively rough landscape, the larger divergence in the local weights induces higher noise. This noise has a landscape smoothing effect, thus stabilizing the convergence. As the training progresses to later stages, gradients become smaller as the models better fit the data, and therefore, the noise reduces accordingly, allowing DSGD to maintain convergence without disrupting optimization. This adaptive regularization has been empirically shown to be more effective than injecting Gaussian noise into CSGD. Zhu et al. (2023) show that DSGD has a generalization advantage over CSGD. They prove that DSGD is asymptotically equivalent to averaged direction sharpness aware minimization (Wen et al., 2022), as the diversity in local weights introduces structured noise. It leads the optimization towards flatter regions of the loss landscape. Importantly, this effect does not diminish with increasing batch sizes, making DSGD more robust and generalizable than CSGD in large batch training. Ye et al. (2025) justify an upper bound for the generalization error in DSGD under data heterogeneity and without the assumption of bounded stochastic gradients. This upper bound reveals that a good generalization in DSGD is favored by lower stochastic noises and reduced data heterogeneity, which correspond to larger batch sizes and more i.i.d. data distributions across nodes. Deng et al. (2023) derive generalization bounds for DSGD that specifically depends on the spectral gap of the communication topology. They show that generalization errors increase as the spectral gap narrows, i.e., as the topology becomes sparser.

3 Decentralized Policy Gradient

Preliminaries We model a cooperative multi-agent reinforcement learning (MARL) problem as a Decentralized Partially Observable Markov Decision Process (Dec-POMDP), defined as

$$\mathcal{M} = (\mathcal{S}, \{\mathcal{A}_i\}_{i=1}^n, P, R, \{\mathcal{O}_i\}_{i=1}^n, \{O_i\}_{i=1}^n, \gamma, n, \rho_0)\,.$$

where n denotes the number of agents, $\mathcal{S}$ is the (global) state space, and ρ_0 is the initial state distribution. The joint action space is $\boldsymbol{a} = (a^1, a^2, \ldots, a^n) \in \prod_{i=1}^n \mathcal{A}_i$, where $\mathcal{A}_i$ is the action space of agent i. The environment transition dynamics are defined by $P(s' \mid s, \boldsymbol{a})$, which gives the probability of transitioning to state s' given the current state s and joint action $\boldsymbol{a}$. The reward function $R(s, \boldsymbol{a})$ provides a shared scalar reward r to all agents. The discount factor is $\gamma \in [0, 1)$. Each agent i receives a local observation $o^i \in \mathcal{O}_i$, where $\mathcal{O}_i$ is its observation space. The observation function $O_i(o^i \mid s)$ defines the probability of agent i observing o^i given the global state s. Let $\boldsymbol{o} = (o^1, \ldots, o^n) \in \prod_{i=1}^n \mathcal{O}_i$ denote the joint observation. Assuming the joint policy $\boldsymbol{\pi}(\boldsymbol{a} \mid \boldsymbol{o}) = \prod_{i=1}^n \pi^i(a^i \mid o^i)$, the objective is to maximize the expected discounted cumulative reward $\mathbb{E}\left[\sum_{t=0}^{\infty} \gamma^t r_t\right]$.

Decentralized Policy Gradient (DecPG) We propose a DSGD-based MARL algorithm, DecPG. To enable that, we simulate MARL as a distributed learning case. Every agent forms a local node with a copy of the initial model θ_0, an independent dataset D_i, and a loss function L_i. At the beginning of every iteration, agents use their local models θ_i to roll out trajectories, forming the local dataset for training. The dataset for agent i at mth iteration is defined as:

$$D_m^i = \{\tau_b^i\}_{b=1}^B,$$

where B is the batch size, and each trajectory τ_b^i of length T is defined as: $\tau_b^i = \{(o_t^i, s_t, a_t^i)\}_{t=0}^T$, where $s_0 \sim \rho_0(s)$, $o_t^i = O_i(s_t)$, $a_t^i \sim \pi^i(a_t^i \mid o_t^i)$, $s_{t+1} \sim P(s_{t+1} \mid s_t, a_t^i, \boldsymbol{a}_t^{-i})$, $\boldsymbol{a}_t^{-i} \sim \boldsymbol{\pi}^{-i}(\boldsymbol{a}_t^{-i} \mid \boldsymbol{o}_t^{-i})$.

Unlike supervised learning, where the local datasets are stationary once defined, the local datasets for agents in MARL have a non-stationary distribution. The local datasets depend on the local policies as well as the influence of other agents' actions. To mitigate the effect of this distribution shift on DSGD, we use MAPPO (Yu et al., 2022) as the backbone because it enforces trust-region control via gradient clipping to make the change in agent policy reasonably small in a local temporal range, and employ the Centralized Training Decentralized Execution (CTDE) (Amato, 2024; Foerster et al., 2018; Sunehag et al., 2017) paradigm to mitigate the non-stationarity caused by inter-agent interaction. With these measures, we make the local data as reasonably stationary as possible. Furthermore, Ye et al. (2025) show that heterogeneous data can slow down the convergence and impair generalization. We thus focus primarily on homogeneous problems, where agents are identical.

The communication topology P for DecPG is defined by a doubly stochastic k-Nearest Neighbor (kNN) graph. Figure 1 illustrates an example when $n = 11$. Intuitively, agents are arranged in a circle, and each agent is connected to its k nearest neighbors. P is an $n \times n$ matrix, where $P_{i,j}$ is the weight of the connection from agent i to agent j. In a kNN topology, $P_{i,j} = 0$ if two agents are disconnected and $P_{i,j} = 1/(k+1)$ if agent i is connected to agent j. For a scenario with n agents, there are $n - 1$ possible kNN topologies. The case $k = 0$ corresponds to a completely disconnected graph, which is equivalent to non-parameter sharing. When $k = n - 1$, the graph is fully connected, corresponding to PS. In this paper, we consider values of k ranging from 1 to $n - 2$, forming an approximately linear progression of spectral gap values from 0 to 1 (Figure 6 in Appendix A.2). The spectral gap is defined as $1 - |\lambda|$, where $|\lambda| = \max_{i \geq 2} |\lambda_i|$ is the second-largest modulus among eigenvalues λ_i of P.

During training, each agent adopts the same loss function but computes it using its own local dataset D_m^i, and the loss is computed as:

$$L_m^i = \frac{1}{B}\frac{1}{T}\sum_{b=1}^{B}\sum_{t=1}^{T} \ell(o_{b,t}^i, s_{b,t}, a_{b,t}^i),$$

where $\ell(\cdot)$ denotes either the policy or critic loss, and $(o_{b,t}^i, s_{b,t}, a_{b,t}^i)$ denotes t-th step in b-th trajectory from D_m^i.

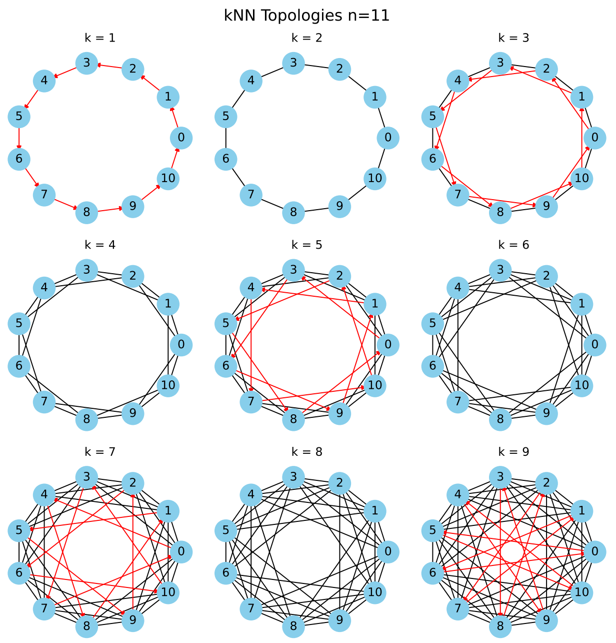

Figure 1: kNN communication topologies for $n = 11$ with $k = 1$ to 9. Black edges indicate bidirectional connections; red edges indicate unidirectional edges.

After gradients being computed locally for all agents, the DSGD mixing is performed for every agent, over itself and its neighbours, defined as:

$$\theta^i_{m+1} = \sum_j^n P_{i,j}\theta^j_m - \eta \cdot \nabla L^i_m(\theta^i_m)$$

This makes DecPG contrary to PS, which averages the gradients of all agents, analogous to CSGD. For instance, in a scenario with 11 agents and a topology with $k = 2$ (Figure 1), during the DSGD mixing step, the updated model weights of agent 0 are given by

$$\theta^0_{m+1} = P_{0,10} \cdot \theta^{10}_m + P_{0,0} \cdot \theta^0_m + P_{0,1} \cdot \theta^1_m - \eta \cdot \nabla L^0_m(\theta^0_m),$$

where $P_{0,10} = P_{0,0} = P_{0,1} = \frac{1}{3}$.

In evaluation, the average model $\theta^{avg}_m = \frac{1}{n}\sum_i^n \theta^i_m$ is used to rollout, following standard practice in DSGD (Zhang et al., 2021; Lian et al., 2017; Ye et al., 2025).

4 Experiments

We use Simple Spread from Multi-Agent Particle Environment (MPE) (Mordatch & Abbeel, 2017) and StarCraft Multi-Agent Challenge (SMAC) (Samvelyan et al., 2019) as the testbeds. Simple Spread is a straightforward task where agents navigate to reach landmarks while avoiding colliding with each other. The reward is easy to interpret, consisting of the agents' distances to landmarks and penalties for collision. We treat Simple Spread as a toy example for its simplicity and interpretability, and use it to identify performance patterns across different algorithms. For Simple Spread, we use scenarios with agent counts ranging from 8 to 12.

On the other hand, SMAC is a widely adopted MARL benchmark featuring challenging micromanagement tasks, where agents control a team of units to defeat the enemies. The reward structure of SMAC is more complicated, involving factors such as ally and enemy health, unit losses, and the winning status. Due to this complexity, we primarily use SMAC to evaluate the overall performance of algorithms rather than to interpret fine-grained trends. In SMAC, we select the homogeneous maps *5m_vs_6m*, *10m_vs_11m*, *27m_vs_30m*, and *6h_vs_8z*, covering a variety of agent counts. These maps are considered challenging as they involve more enemies than agents, thus requiring more precise coordination.

DecPG is tested under different kNN communication topologies that approximately evenly span the spectral gap, ranging from 0 to 1. For instance, we select 4 topologies $k = 2, 4, 6, 8$ for $n = 10$, with spectral gaps around 0.13, 0.35, 0.63 and 0.89 respectively, roughly spanning the entire spectral gap linearly.

We compare DecPG with the standard PS baseline. Additionally, we include a PS variant with entropy regularization, as we observe that DecPG tends to induce more exploration reflected by higher policy entropy than standard PS (see Appendix A.3). We evaluate whether DecPG outperforms entropy regularization, a commonly used technique in MARL.

All experiments use vanilla SGD as the optimizer with full-batch training. We adopt a neural network architecture consisting of 3 linear layers, followed by a GRU layer, another linear layer, and finally an output layer, for both the actor and critic. For details on other hyperparameters, please refer to Appendix A.1.

To evaluate DecPG, we consider the following metrics. First, we examine the training performance (average episode reward), which refers to the policy's performance on the same environment as in training, but evaluated with different random seeds and using the deterministic average policy.

Since the difference in MARL environments across seeds is negligible for evaluating generalization, we adopt a modified version of the training environment for testing, where additional stochasticity is introduced. We inject Gaussian noise into the observation space to simulate real-world imperfections, using a mean of 0 and a standard deviation equal to c times the sample standard deviation. The perturbations can be regarded as the sensor noise in reality. A well-generalized policy should exhibit minimal performance degradation under such perturbations, indicating robustness beyond memorization of training states. We also introduce stochasticity in the action space. This models real-world actuation uncertainty. For example, in a robot navigation task, practical factors such as friction or small obstacles (e.g., pebbles) can cause deviations from intended trajectories. We simulate such effects by injecting random perturbations into the action space. Since the environments are discrete, we assign a small probability ε for an action to be replaced with a random one. This tests the policy's robustness by forcing it to handle unanticipated deviations, implicitly requiring it to have adequately explored the environment during training. A robust policy should still be able to recover and follow near-optimal trajectories despite such disturbances.

These modifications ensure that the test environment does not follow the exact same distribution as the training environment, while still preserving the core task, enabling evaluation of the policy's ability to generalize without changing the underlying problem.

We regard the test performance (test average episode reward) as the primary metric for the generalization power of a policy. Generalization gap is provided as an additional metric for generalization, defined as the difference between test and train performance. This gap reflects the extent to which performance degrades when transitioning from the training to the test environment. A higher test performance and a smaller generalization gap indicate stronger generalization.

Additionally, we visualize the reward and loss landscapes of the learned policies in 3D. This is done by selecting two orthonormal directions in the policy parameter space and perturbing the policy along those directions. These visualizations provide qualitative insight into generalization from the perspective of landscape flatness.

All experiments were run for 3 seeds, on Google TPU v4-8. Results shown in Figures 2, 3, and 4 are the median values. Shaded regions in Figure 2 display the 95% confidence zone. Bars in Figure 3 show the standard deviation.

5 Results and Findings

Through comprehensive empirical evaluation, we have the following findings.

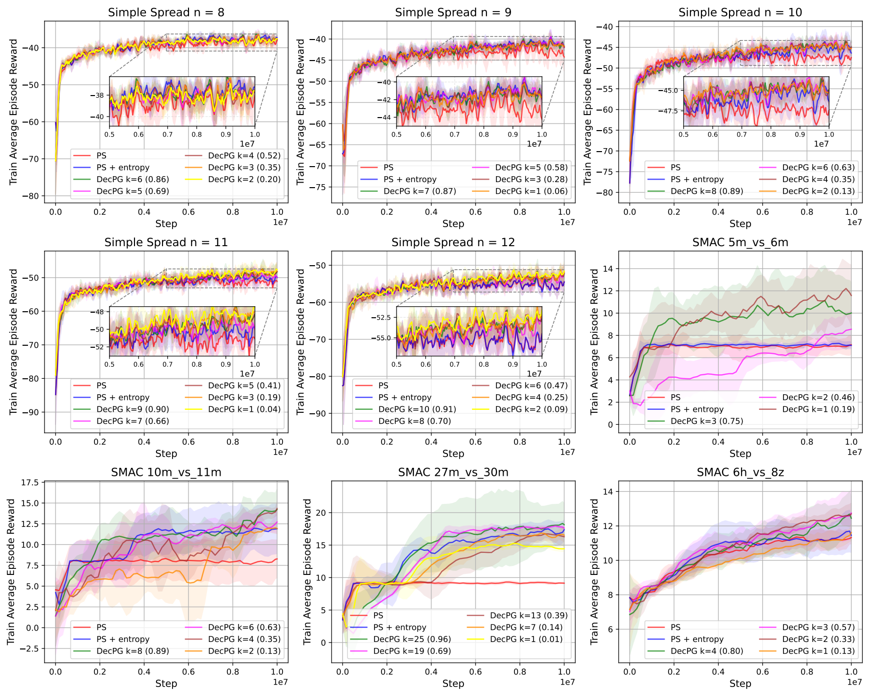

Figure 2: Training average episode rewards on MPE Simple Spread and SMAC, evaluated using deterministic policies. We compare PS, PS with entropy regularization (PS+entropy), and DecPG with different topologies (DecPG k=x). For DecPG, the value x in parentheses indicates the spectral gap of the corresponding topology.

5.1 DecPG achieves better convergence and exploration than the PS baselines during training.

Figure 2 shows the average episode rewards obtained using the deterministic policy during training. In Simple Spread scenarios with $n = 9$–12, the performance of PS plateaus early during training. In contrast, across all scenarios, DecPG consistently maintains an upward trend and outperforms PS by the end of training.

By analyzing the evolution of policy entropy (Figure 7), we observe that DecPG's entropy decreases steadily, whereas PS exhibits a much faster drop. We deduce that the noise introduced by DecPG slows convergence, thereby encouraging more exploration.

Entropy regularization helps PS achieve a similar level of exploration (e.g., $n = 8, 9, 10$); however, this effect diminishes as the number of agents increases (e.g., $n = 11, 12$).

The training performance in SMAC aligns with the findings from Simple Spread (Figure 2). Across all maps, DecPG consistently outperforms PS, which again exhibits a plateauing trend during training. PS with entropy regularization performs more competitively than in Simple Spread. It matches DecPG with $k = 2$ in 10m_vs_11m, $k = 1$ in 6h_vs_8z, and even surpasses DecPG with $k = 13, 7, 1$ in 27m_vs_30m. Nevertheless, the best performance on each map is still achieved by a DecPG policy.

5.2 DecPG demonstrates better generalization than PS.

Figure 3 shows the test average episode rewards, evaluated using the final converged policies of the PS and DecPG baselines. In all Simple Spread scenarios, standard PS consistently performs the worst. PS with entropy regularization achieves the best test performance in the $n = 8$ scenario and performs comparably to DecPG when $n = 9$. However, as the number of agents increases, it results in lower test rewards than DecPG policies, and the performance gap widens.

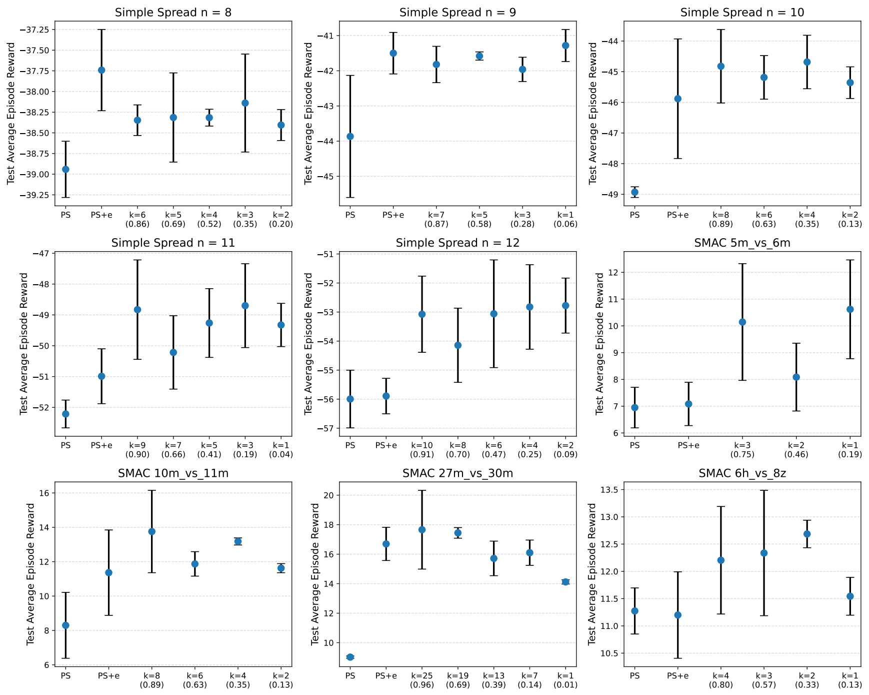

Figure 3: Test average episode rewards of the final deterministic policies on MPE Simple Spread and SMAC.

As for the test performance in SMAC (Figure 3), we observe a generally increasing trend in test performance, with PS performing the worst, followed by PS with entropy regularization, and DecPG achieving the highest performance.

Across all scenarios except Simple Spread $n = 8$, DecPG consistently outperforms the PS baselines in terms of test performance, highlighting the generalization advantage of DSGD-style updates over CSGD.

5.3 Relationship between DecPG performance and topology sparsity.

In terms of training rewards (Figure 2), DecPG with different topologies performs similarly in most scenarios, without exhibiting a clear trend with respect to topology sparsity. However, it is noteworthy that in Simple Spread, the sparsest topology achieves the highest reward for $n = 11$ and 12, whereas in SMAC, these topologies lead to performance degradation, particularly in *6h_vs_8z*, *10m_vs_11m*, and *27m_vs_30m*.

We observe that sparser topologies tend to achieve better test performance (Figure 3). In most scenarios, the highest test performance of DecPG is achieved with the sparsest or the second sparsest topologies. However, in *27m_vs_30m* and *6h_vs_8z*, DecPG policies with the smaller ks result in a drop in performance. This is consistent with the findings from training performance and reconfirms that overly sparse topologies can degrade performance in difficult tasks.

We interpret these findings in light of the theoretical results from distributed learning. Deng et al. (2023) prove that generalization error increases as the topology becomes sparser, while Ye et al. (2025) justify that data heterogeneity across nodes can deteriorate generalization. We deduce that, in a more difficult environment like SMAC, overly sparse topologies slow down the consensus between nodes, which exacerbates data heterogeneity, ultimately resulting in lower generalization. Based on our findings, we empirically recommend avoiding extremely sparse topologies (e.g., those with a spectral distance ≤ 0.13) to prevent the unexpected performance degradation in practice.

Generalization gaps are shown in Figure 4. Across all Simple Spread scenarios, we observe a decreasing trend in generalization gaps as topology sparsity increases (i.e., as k decreases), though minor fluctuations exist. This suggests that generalization improves with increased sparsity.

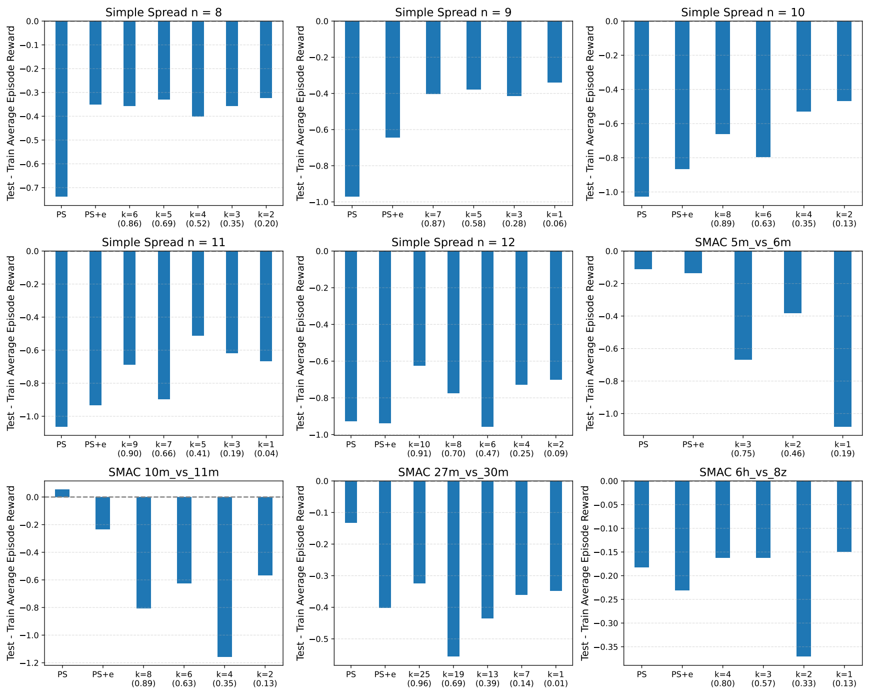

Figure 4: Generalization gap on MPE Simple Spread and SMAC, computed as the difference between test and training rewards.

Unfortunately, we do not observe a similar trend in the SMAC scenarios (Figure 4). Instead, we find that the generalization gaps are more closely correlated with absolute test performance. Specifically, higher test performance is associated with larger generalization gaps. We attribute this to the nature of the selected SMAC maps, which involve imbalanced ally and enemy team sizes and demand more fine-grained coordination among agents to defeat larger numbers of opponents. As a result, perturbations in the test environment tend to have a more catastrophic impact on well-performing policies than on those that already perform relatively poorly. Although this effect dominates the generalization gap patterns and obscures the trend observed in Simple Spread, the test performance results presented earlier remain sufficient to reveal the generalization capabilities of DecPG under different topologies.

Overall, the results show that while different topologies often perform similarly during training, sparser topologies tend to produce more generalized and robust policies. However, overly sparse topologies should be avoided to prevent unexpected performance degradation.

5.4 DecPG achieves flatter reward landscapes as topology becomes sparser.

Figure 5a present the 3D visualizations of the reward landscapes for the final converged policies of the DecPG and PS baselines in the Simple Spread $n = 10$ scenario. Visually, the reward landscapes for the PS and PS with entropy regularization baselines show a significant drop along the negative β direction, indicating that these policies are highly sensitive to perturbations. In contrast, for DecPG, this drop gradually vanishes as k decreases from 8 to 2, eventually resulting in an almost flat landscape. This suggests that DecPG with sparser topologies yields more robust policies.

This trend is also reflected in the reward histograms (see Appendix A.4, Figure 8a). The PS baselines exhibit long left tails, indicating that most perturbations lead to a drop in reward. In comparison, DecPG produces much shorter tails, and these tails become less pronounced as k decreases, reinforcing the visual observation from the 3D plots.

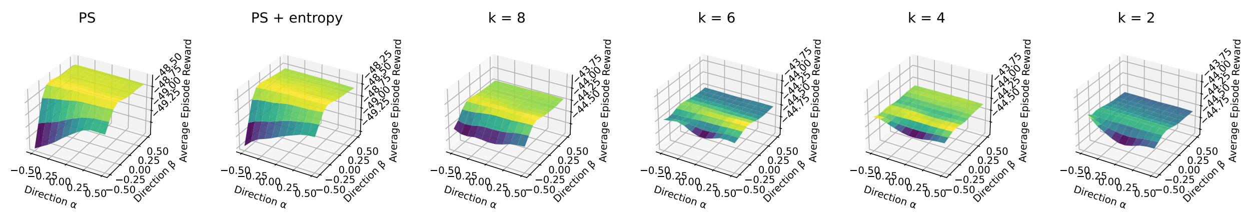

(a) Average episode reward landscape surface

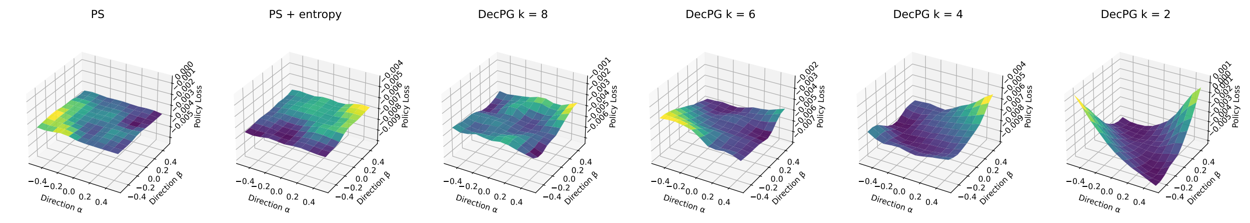

(b) Policy loss landscape surface

Figure 5: Visualization of reward and loss landscapes in MPE Simple Spread $n = 10$, for PS, PS with entropy regularization (PS+entropy), and DecPG with different topologies (DecPG k=x). Subfigures **(a)** and **(b)** show 3D surfaces of the reward and loss with respect to perturbations in two orthonormal directions of the parameter space.

Figure 5b shows the loss landscapes for the Simple Spread $n = 10$ scenario. Contrary to findings in supervised learning (Zhu et al., 2023), DecPG does not exhibit flatter loss landscapes as topology becomes sparser. This is because the DecPG policies converge to different final policies, corresponding to different local optima under different data regimes, thus making cross-policy comparisons of loss landscapes potentially invalid.

To sum up, the gaps between DecPG and PS in both training and testing confirm that PS suffers from similar optimization issues as CSGD. In contrast, DecPG, based on DSGD, demonstrates stronger exploration, convergence, and generalization compared to the PS baselines, proving itself as an effective solution to these problems. The noise inherent in DSGD implicitly encourages exploration, which is more effective than entropy regularization in most scenarios. This noise guides the policy toward flatter and more robust optima in the reward landscape, thereby achieving better convergence and generalization.

6 Conclusion

In conclusion, this paper proposed a DSGD-based MARL algorithm, DecPG, which leverages decentralized updates to improve generalization and convergence. We conducted an empirical analysis comparing DecPG with its CSGD counterpart, PS, in the MPE Simple Spread and SMAC environments across homogeneous tasks. Our results show that DecPG outperforms PS in the training environment and achieves superior test performance in most scenarios, including over PS with entropy regularization. This supports our conclusion that PS inherits generalization issues from CSGD, and that DecPG (DSGD) offers an effective solution.

To further assess generalization, we presented generalization gaps and visualizations and histograms of reward landscapes for DecPG and PS baselines. These results illustrate that as DecPG topology becomes sparser the generalization gaps decrease and the reward landscapes become flatter.

Future work includes extending this research by incorporating advanced optimizers, such as momentum-based methods like Adam, which are critical for training modern neural networks like Transformers. Additionally, this paper simulates decentralized training under a single-worker CTDE framework. Therefore, future studies should explore fully distributed training setups to assess the practical advantages of DecPG. Finally, since this paper primarily focused on empirical analysis, theoretical justifications are also desirable to better understand the optimization behavior in MARL.

References

Christopher Amato. An introduction to centralized training for decentralized execution in cooperative multi-agent reinforcement learning. *arXiv preprint arXiv:2409.03052*, 2024.

Filippos Christianos, Georgios Papoudakis, Muhammad A Rahman, and Stefano V Albrecht. Scaling multi-agent reinforcement learning with selective parameter sharing. In *International Conference on Machine Learning*, pp. 1989–1998. PMLR, 2021.

Xiangxiang Chu and Hangjun Ye. Parameter sharing deep deterministic policy gradient for cooperative multi-agent reinforcement learning. *arXiv preprint arXiv:1710.00336*, 2017.

Ofer Dekel, Ran Gilad-Bachrach, Ohad Shamir, and Lin Xiao. Optimal distributed online prediction using mini-batches. *The Journal of Machine Learning Research*, 13(1):165–202, 2012.

Xiaoge Deng, Tao Sun, Shengwei Li, and Dongsheng Li. Stability-based generalization analysis of the asynchronous decentralized sgd. In *Proceedings of the AAAI conference on artificial intelligence*, volume 37, pp. 7340–7348, 2023.

Jakob Foerster, Gregory Farquhar, Triantafyllos Afouras, Nantas Nardelli, and Shimon Whiteson. Counterfactual multi-agent policy gradients. In *Proceedings of the AAAI conference on artificial intelligence*, volume 32, 2018.

Priya Goyal, Piotr Dollár, Ross Girshick, Pieter Noordhuis, Lukasz Wesolowski, Aapo Kyrola, Andrew Tulloch, Yangqing Jia, and Kaiming He. Accurate, large minibatch sgd: Training imagenet in 1 hour. *arXiv preprint arXiv:1706.02677*, 2017.

Jayesh K Gupta, Maxim Egorov, and Mykel Kochenderfer. Cooperative multi-agent control using deep reinforcement learning. In *International conference on autonomous agents and multiagent systems*, pp. 66–83. Springer, 2017.

Sepp Hochreiter and Jürgen Schmidhuber. Flat minima. *Neural computation*, 9(1):1–42, 1997.

Stanislaw Jastrzebski, Zachary Kenton, Devansh Arpit, Nicolas Ballas, Asja Fischer, Yoshua Bengio, and Amos Storkey. Three factors influencing minima in sgd. *arXiv preprint arXiv:1711.04623*, 2017.

Nitish Shirish Keskar, Dheevatsa Mudigere, Jorge Nocedal, Mikhail Smelyanskiy, and Ping Tak Peter Tang. On large-batch training for deep learning: Generalization gap and sharp minima. *arXiv preprint arXiv:1609.04836*, 2016.

Woojun Kim and Youngchul Sung. Parameter sharing with network pruning for scalable multi-agent deep reinforcement learning. *arXiv preprint arXiv:2303.00912*, 2023.

Anastasia Koloskova, Nicolas Loizou, Sadra Boreiri, Martin Jaggi, and Sebastian Stich. A unified theory of decentralized sgd with changing topology and local updates. In *International conference on machine learning*, pp. 5381–5393. PMLR, 2020.

Xinran Li, Ling Pan, and Jun Zhang. Kaleidoscope: Learnable masks for heterogeneous multi-agent reinforcement learning. *Advances in Neural Information Processing Systems*, 37:22081–22106, 2024.

Xiangru Lian, Ce Zhang, Huan Zhang, Cho-Jui Hsieh, Wei Zhang, and Ji Liu. Can decentralized algorithms outperform centralized algorithms? a case study for decentralized parallel stochastic gradient descent. *Advances in neural information processing systems*, 30, 2017.

Igor Mordatch and Pieter Abbeel. Emergence of grounded compositional language in multi-agent populations. *arXiv preprint arXiv:1703.04908*, 2017.

Haoyuan Qin, Zhengzhu Liu, Chenxing Lin, Chennan Ma, Songzhu Mei, Siqi Shen, and Cheng Wang. Gradps: Resolving futile neurons in parameter sharing network for multi-agent reinforcement learning. In *Forty-second International Conference on Machine Learning*, 2025.

Tabish Rashid, Mikayel Samvelyan, Christian Schroeder De Witt, Gregory Farquhar, Jakob Foerster, and Shimon Whiteson. Monotonic value function factorisation for deep multi-agent reinforcement learning. *Journal of Machine Learning Research*, 21(178):1–51, 2020.

Mikayel Samvelyan, Tabish Rashid, Christian Schroeder de Witt, Gregory Farquhar, Nantas Nardelli, Tim G. J. Rudner, Chia-Man Hung, Philiph H. S. Torr, Jakob Foerster, and Shimon Whiteson. The StarCraft Multi-Agent Challenge. *CoRR*, abs/1902.04043, 2019.

Peter Sunehag, Guy Lever, Audrunas Gruslys, Wojciech Marian Czarnecki, Vinicius Zambaldi, Max Jaderberg, Marc Lanctot, Nicolas Sonnerat, Joel Z Leibo, Karl Tuyls, et al. Value-decomposition networks for cooperative multi-agent learning. *arXiv preprint arXiv:1706.05296*, 2017.

Justin K Terry, Nathaniel Grammel, Sanghyun Son, Benjamin Black, and Aakriti Agrawal. Revisiting parameter sharing in multi-agent deep reinforcement learning. *arXiv preprint arXiv:2005.13625*, 2020a.

Justin K Terry, Nathaniel Grammel, Sanghyun Son, Benjamin Black, and Aakriti Agrawal. Revisiting parameter sharing in multi-agent deep reinforcement learning. *arXiv preprint arXiv:2005.13625*, 2020b.

Xihuai Wang, Zheng Tian, Ziyu Wan, Ying Wen, Jun Wang, and Weinan Zhang. Order matters: Agent-by-agent policy optimization. *arXiv preprint arXiv:2302.06205*, 2023.

Kaiyue Wen, Tengyu Ma, and Zhiyuan Li. How sharpness-aware minimization minimizes sharpness? In *The Eleventh International Conference on Learning Representations*, 2022.

Haoxiang Ye, Tao Sun, and Qing Ling. Generalization guarantee of decentralized learning with heterogeneous data. In *ICASSP 2025-2025 IEEE International Conference on Acoustics, Speech and Signal Processing (ICASSP)*, pp. 1–5. IEEE, 2025.

Yang You, Igor Gitman, and Boris Ginsburg. Large batch training of convolutional networks. *arXiv preprint arXiv:1708.03888*, 2017.

Chao Yu, Akash Velu, Eugene Vinitsky, Jiaxuan Gao, Yu Wang, Alexandre Bayen, and Yi Wu. The surprising effectiveness of ppo in cooperative multi-agent games. *Advances in neural information processing systems*, 35:24611–24624, 2022.

Wei Zhang, Xiaodong Cui, Ulrich Finkler, George Saon, Abdullah Kayi, Alper Buyuktosunoglu, Brian Kingsbury, David Kung, and Michael Picheny. A highly efficient distributed deep learning system for automatic speech recognition. *arXiv preprint arXiv:1907.05701*, 2019.

Wei Zhang, Mingrui Liu, Yu Feng, Xiaodong Cui, Brian Kingsbury, and Yuhai Tu. Loss landscape dependent self-adjusting learning rates in decentralized stochastic gradient descent. *arXiv preprint arXiv:2112.01433*, 2021.

Yifan Zhong, Jakub Grudzien Kuba, Xidong Feng, Siyi Hu, Jiaming Ji, and Yaodong Yang. Heterogeneous-agent reinforcement learning. *Journal of Machine Learning Research*, 25(32):1–67, 2024.

Tongtian Zhu, Fengxiang He, Kaixuan Chen, Mingli Song, and Dacheng Tao. Decentralized sgd and average-direction sam are asymptotically equivalent. In *International Conference on Machine Learning*, pp. 43005–43036. PMLR, 2023.

A Appendix

A.1 Hyper-parameters

This section provides the hyperparameter configurations used for training the PS, PS+entropy, and DecPG policies across the MPE Simple Spread and SMAC environments. Table 1 summarizes the hyperparameters that are shared across all tasks and methods. Table 2 details the task-specific and algorithm-specific hyperparameters used in SMAC for each method.

Table 1: Shared hyperparameter configurations for MPE Simple Spread and SMAC environments.

Hyperparameter	MPE Simple Spread	SMAC
Learning rate (lr)	1e-2	—
Minimum lr	1e-3	—
lr decay	Linear	Linear
Number of mini-batches	1	1
Batch size	800	3200
PPO epochs	10	—
Clipping parameter	0.2	—
Entropy coefficient	1e-3	5e-3
Max gradient norm	10	10
Hidden layer size	64	64
Test Environment σ	0.2	0.1
Test Environment c	0.2	0.01

Table 2: Hyperparameter configurations used for SMAC environments across PS, PS+entropy, and DecPG.

	5m_vs_6m			10m_vs_11m			27m_vs_30m			6h_vs_8z		
	PS	PS+entropy	DecPG	PS	PS+entropy	DecPG	PS	PS+entropy	DecPG	PS	PS+entropy	DecPG
lr	1e-2	1e-2	1e-1	1e-2	1e-2	1e-1	1e-1	1e-1	3e-1	1e-1	1e-1	3e-1
min lr	1e-3	1e-3	1e-2	1e-3	1e-3	1e-2	1e-2	1e-2	3e-2	1e-2	1e-2	3e-2
clip param		0.05			0.2			0.2			0.2	
ppo epoch		10			10			5			5	

A.2 Spectral Gap

The spectral gap of a doubly stochastic matrix P is defined as the difference between its largest eigenvalue (which is 1) and the second-largest eigenvalue in modulus. The formula is given by

$$\text{Spectral Gap} := 1 - \max_{i \geq 2} |\lambda_i|$$

where λ_i are the eigenvalues of P. An example of the spectral gap values for kNN topologies with 11 agents is shown in Figure 6

A.3 Policy Entropy

Figure 7 shows the policy entropy of DecPG with different topologies and the PS baselines during training. In the majority of scenarios, DecPG policies maintain higher entropy levels than PS, indicating greater exploration. In contrast, PS with entropy regularization successfully increases exploration, often reaching entropy levels comparable to or higher than those of DecPG.

A.4 Landscape Histograms

Figure 8 shows the histograms of the reward and loss landscapes corresponding to Figure 5. Longer tails indicate sharper landscapes, while shorter tails suggest flatter ones.

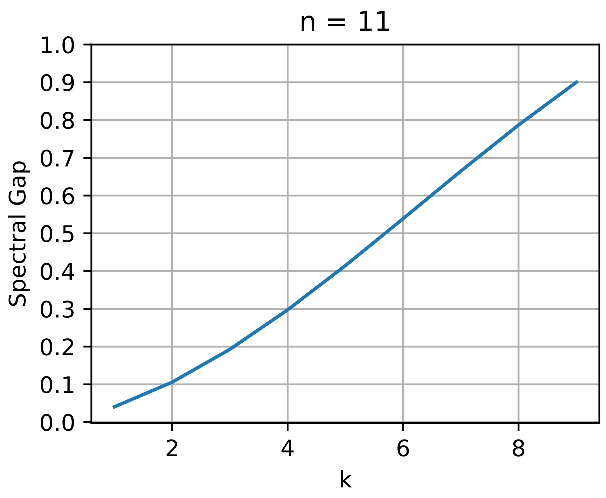

Figure 6: Spectral gaps for $n = 11$ with $k = 1$ to 9

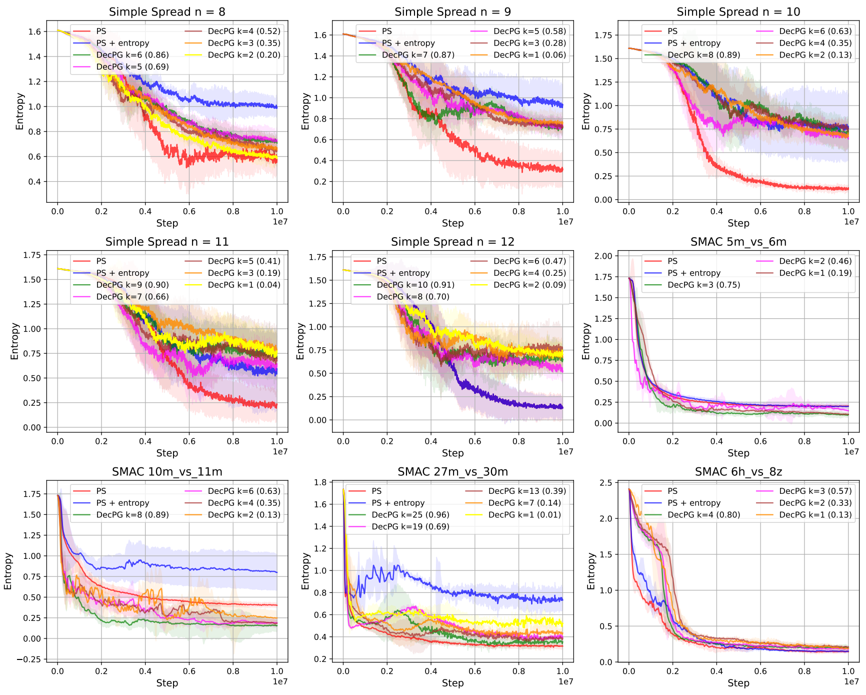

Figure 7: Policy entropy for PS, PS with entropy regularization and DecPG with different topologies.

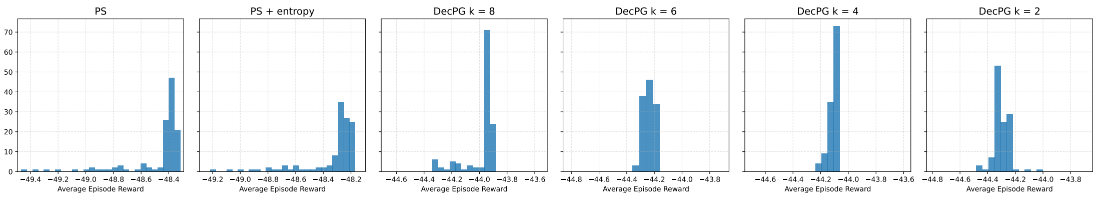

(a) Average episode reward histogram

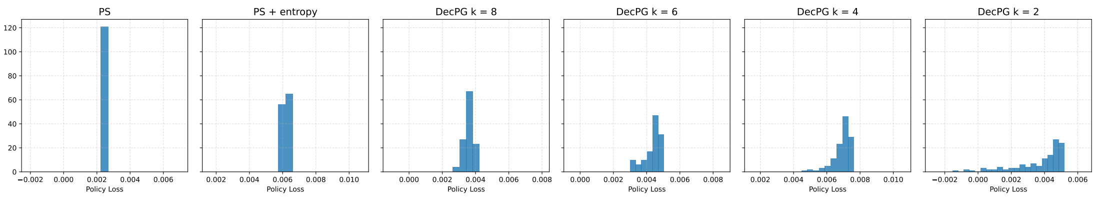

(b) Policy loss landscape histogram

Figure 8: Visualization of reward and loss landscapes in MPE Simple Spread $n = 10$, for PS, PS with entropy regularization (PS+entropy), and DecPG with different topologies (DecPG k=x). Subfigures **(a)** and **(b)** present the histograms of the same landscape values.